

Optimization of a Defected Ground Structure to Improve Electromagnetic Bandgap Performance

Manseok Kwon¹ · Myunghoi Kim² · Dong Gun Kam^{1,*}

Abstract

A dispersion analysis is performed to estimate the stopband characteristics of electromagnetic bandgap (EBG) structures with defected ground structures (DGS) of various shapes. Design guidelines are suggested for both elliptical and rectangular DGS patterns that result in a maximum stopband bandwidth for a given perforation area. This method provides a basis for numerical optimization techniques that can be used in synthesizing DGS shapes to meet bandgap requirements and layout constraints.

Key Words: Defected Ground Structure (DGS), Dispersion Analysis, Electromagnetic Bandgap (EBG), Power/Ground Noise.

I. INTRODUCTION

In high-speed printed circuit boards (PCBs), the propagation of power/ground (P/G) noise causes a significant degradation of signal integrity. Today, data rates are continuously increasing, so noise coupling through the P/G planes occurs over a wide range of frequencies. Therefore, wideband suppression of P/G noise coupling is an essential requirement for high-speed PCBs. Electromagnetic bandgap (EBG) structures have emerged as an effective solution because they have wide stopband bandwidths, high stopband attenuation, and are easily integrated with PCBs [1]. Various techniques have been proposed to improve the noise-suppression characteristics while minimizing the size of EBG structures; these include the use of high dielectric constant materials, multivias structures, cascaded EBG cells, and defected ground structures (DGSs) [1]. The employment of DGSs has a distinctive advantage over the other methods: design modi-

fications (i.e., removing a part of a ground plane) add no cost.

In [2], circular DGS patterns are proposed for further improvement of the stopband bandwidth with a smaller perforation area. An analytical model is also presented to determine the bandgap characteristics of the proposed structure. The method proposed in the present study involves the segmentation of a transmission line with an arbitrary characteristic impedance into multiple sections so that the characteristic impedance can be regarded as a linear function of x (the wave propagation axis) in each section (i.e., applying the piecewise linear approximation). Good model-hardware correlation and flexible simulation setups allow us to explore a variety of DGS shapes in order to determine the best DGS pattern for maximizing the stopband bandwidth.

II. OPTIMIZATION OF DGS SHAPES

The proposed analytical method considers two lower quasi-

Manuscript received November 3, 2014 ; Revised December 2, 2014 ; Accepted December 12, 2014. (ID No. 20141103-054f)

¹Department of Electronics Engineering, Ajou University, Suwon, Korea.

²Electronics and Telecommunications Research Institute (ETRI), Daejeon, Korea.

*Corresponding Author: Dong Gun Kam (e-mail: kam@ajou.ac.kr)

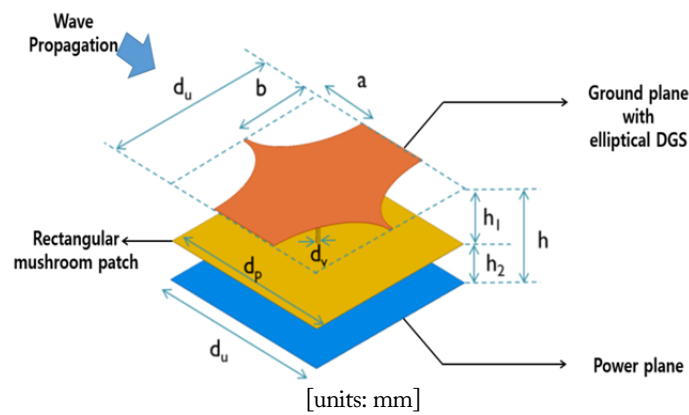
This is an Open-Access article distributed under the terms of the Creative Commons Attribution Non-Commercial License (<http://creativecommons.org/licenses/by-nc/3.0>) which permits unrestricted non-commercial use, distribution, and reproduction in any medium, provided the original work is properly cited.

© Copyright The Korean Institute of Electromagnetic Engineering and Science. All Rights Reserved.

TEM modes and estimates the start and stop bandgap frequencies (f_l, f_h) with reasonable accuracy when compared to full-wave simulations. The proposed method allows rapid analysis of various DGS shapes at the early stages of the design process.

Fig. 1 shows a mushroom-type EBG structure with elliptical DGS patterns. It consists of three metal layers: a dedicated power plane (bottom), EBG patches (middle), and an elliptical DGS (top). An FR-4 substrate is used as a dielectric material ($\epsilon_r = 4.4, \tan\delta = 0.02$). Fig. 2 shows a dispersion diagram calculated using the proposed method, and the stopband ranges from 0.75 to 4.71 GHz. Fig. 3 shows a full-wave simulation result of the same elliptical DGS (Fig. 1). The stopband (-30 dB suppression level) ranges from 0.70 to 3.95 GHz. The proposed method analyzes a unit cell using the periodic boundary conditions (i.e., assuming an infinite array), whereas the full-wave simulation model is made of 3×7 unit cells. Compared with a circular DGS, the elliptical DGS (not yet optimized) has a slightly improved suppression bandwidth.

Next, the dimensions (a and b in Fig. 1) of the elliptical DGS are changed such that its perforation area remains the same



a	b	d_u	d_p	h_1	h_2	d_v
3	5	10.2	10	0.8	0.1	0.2

Fig. 1. Unit cell for an electromagnetic bandgap with elliptical defected ground structure (DGS) patterns.

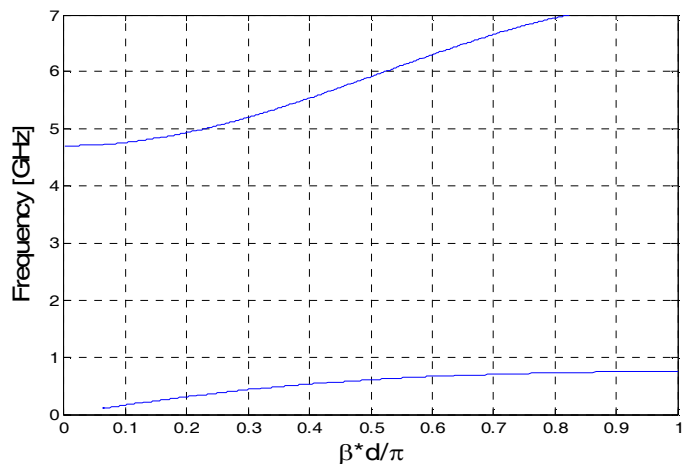


Fig. 2. Dispersion diagram of the structure shown in Fig. 1.

(50%). In Fig. 4, the stopband bandwidth widens as b increases and a decreases. In other words, for a fixed perforation area, aligning the major axis of an ellipse perpendicular to a noise-propagating direction is advantageous.

Two rectangular DGS patterns are then compared to determine whether the same principle applies to other DGS shapes, as shown in Figs. 5 and 6: one with $a = 2.5$ mm and $b = 5$ mm, and the other with $a = 5$ mm and $b = 2.5$ mm. The other dimensions remain the same as in Fig. 1. The first shape has a stopband from 3.14 to 12.71 GHz, while the second has an almost zero stopband. Again, the longer side of a rectangle should be placed perpendicular to the noise-propagating direction.

Next, we change the unit cell size (d_u), maximize b ($b = d_u / 2 - 0.1$), and determine a , such that the perforation area remains

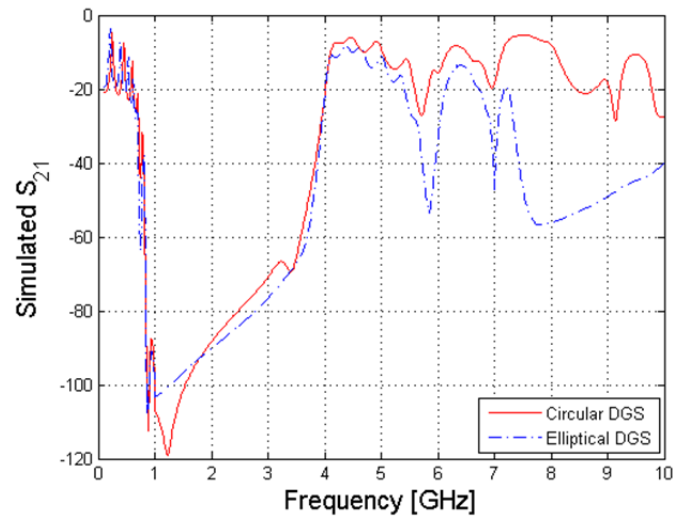


Fig. 3. Influence of defected ground structure (DGS) shape variation on bandgap width.

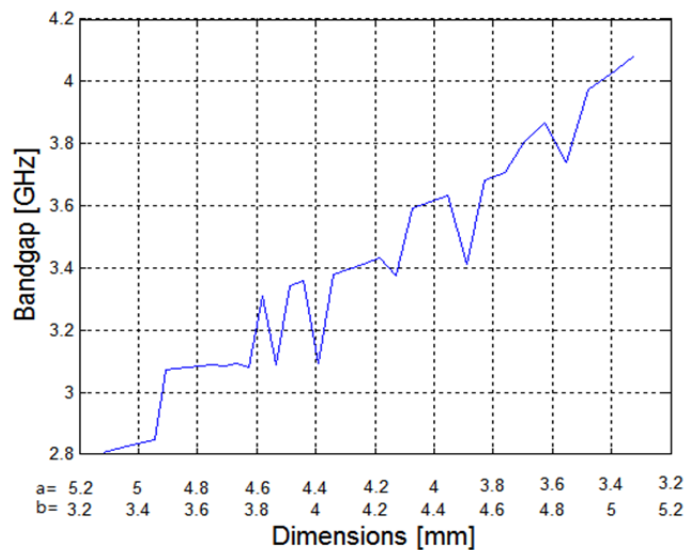


Fig. 4. Influence of defected ground structure shape variation on bandgap width.

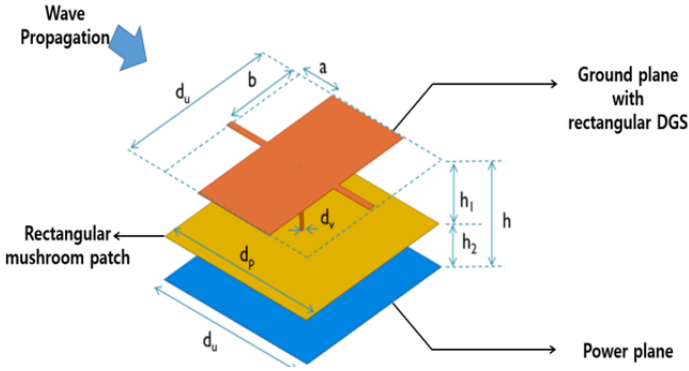


Fig. 5. Unit cell for an electromagnetic bandgap with rectangular defected ground structure (DGS) patterns.

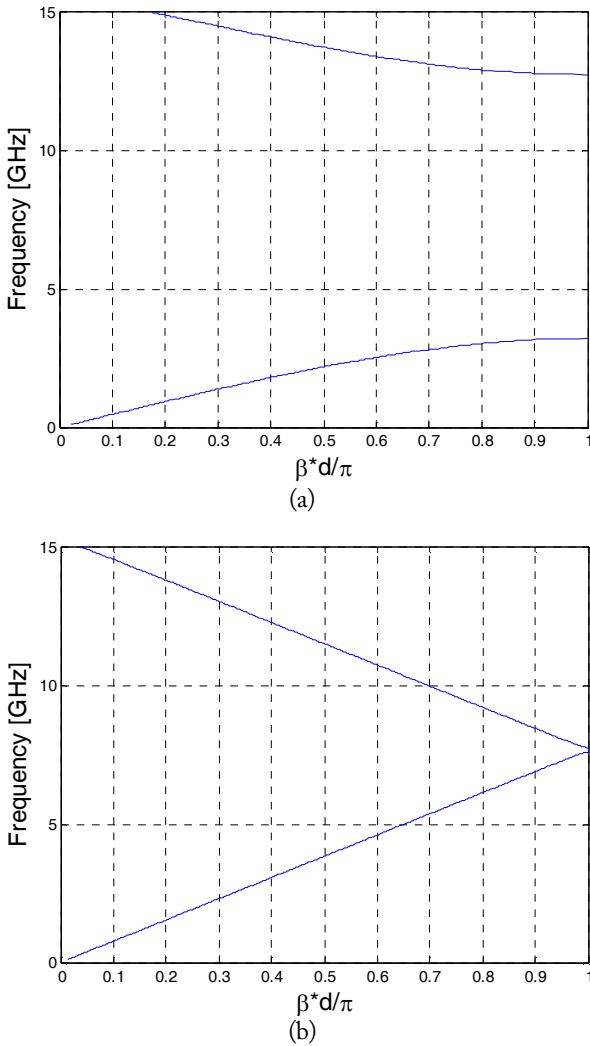


Fig. 6. Dispersion diagram of the structure shown in Fig. 5: (a) $a = 2.5$ mm, $b = 5$ mm, and (b) $a = 5$ mm, $b = 2.5$ mm.

50%. Fig. 7 shows that f_L , f_H , and the stopband bandwidth all decrease as the unit cell becomes larger. An EBG without a mushroom-type patch has much higher f_L and f_H , but the tendency remains the same. Filling a given EBG area with more pieces of a smaller unit cell is advantageous. This also improves

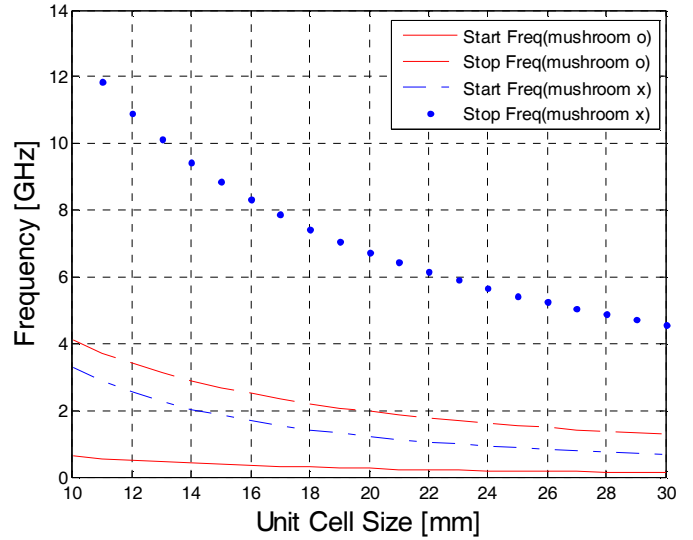


Fig. 7. Effect of unit cell size on start and stop bandgap frequencies.

periodicity, so that the stopband characteristics are closer to the ideal case. Note that the dispersion analysis assumes that an infinite number of EBG cells are placed.

III. CONCLUSION

We extend the analytical method presented in [2] to explore a variety of DGS shapes in the search for better stopband characteristics. The data presented here do not necessarily represent the optimum achievable bandgap performance for each DGS pattern; however, the analysis procedure provides a basis for numerical optimization techniques that can be used in synthesizing DGS shapes that will meet existing bandgap requirements and layout constraints.

This work was supported by the ICT R&D Program of MSIP/IITP (No. 14-911-01-001, Development of quasi-millimeter-wave channel-adaptive antennas and transceivers).

REFERENCES

- [1] M. Kim, K. Koo, C. Hwang, Y. Shim, J. Kim, and J. Kim, "A compact and wideband electromagnetic bandgap structure using a defected ground structure for power/ground noise suppression in multilayer packages and PCBs," *IEEE Transactions on Electromagnetic Compatibility*, vol. 54, no. 3, pp. 689–695, Jun. 2012.
- [2] M. Kim and D. G. Kam, "A wideband and compact EBG structure with a circular defected ground structure," *IEEE Transactions on Components, Packaging and Manufacturing Technology*, vol. 4, no. 3, pp. 496–503, Mar. 2014.